JOURNAL OF MATERIALS SCIENCE **36** (2001) 5927–5934

Corrosion resistance of Cr_2O_3-Al_2O_3 ceramics by molten sodium sulphate–vanadium pentoxide

T. HIRATA
Yokohama Research and Development Center, Mitsubishi Heavy Industries, Ltd., 12, Nishiki-cho, Naka-ku, Yokohama, 231-8715, Japan
E-mail: takehiko_hirata@d.ydmw.mhi.co.jp

K. AKIYAMA, H. YAMAMOTO
Advanced Technology Research Center, Mitsubishi Heavy Industries, Ltd., 8-1 Sachiura 1-chome, Kanazawa-ku, Yokohama, 236-8515, Japan

This report describes an investigation of the hot corrosion resistance of Cr_2O_3-Al_2O_3 ceramics in V_2O_5-Na_2SO_4 molten salt. Adding Cr_2O_3 to Al_2O_3 improves the hot corrosion resistance of Al_2O_3 ceramics, and thickness of the damage zone depends on the sintering temperature and the Cr_2O_3 content. Corrosion of the Cr_2O_3-Al_2O_3 ceramics is caused by the formation of a liquid of the dissolved Na_2O-V_2O_5-$(Al,Cr)_2O_3$ system and by dissolution of the Cr_2O_3-Al_2O_3 ceramics into this liquid. The corrosion rate of the Cr_2O_3-Al_2O_3 ceramics becomes smaller than that of the Al_2O_3 ceramics because dissolution rate of grains into the liquid phase occurring in grain boundaries decreases, compared with the Al_2O_3 ceramics. If the sintering temperature is elevated, grain growth would occur to enhance the corrosion resistance of the ceramics.

1. Introduction

Ceramic materials have the potential to be used in high-temperature components that are exposed to molten-salts because of their high resistance to the molten salt corrosion [1]. There are reports on the corrosion behavior in sulfate of non-oxide ceramics such as Si_3N_4 and SiC, used for gas turbines, etc. [2–4].

Research on the corrosion behavior of oxides in molten salts has principally been concerned with ZrO_2 which has an excellent heat resistance and is used as a thermally sprayed coating [5–12]. Bratton and Lau [6], studied the corrosion of Y_2O_3-stabilized ZrO_2 (YSZ) ceramics in molten salt containing V_2O_5 and concluded that ZrO_2 is de-stabilized due to the formation of YVO_4 which result in corrosion. Watanabe and Chigasaki [7], conducted a corrosion test on CaO-stabilized ZrO_2 in Na_2SO_4-25wt%NaCl and confirmed that de-stabilization due to the formation of $CaSO_4$ causes corrosion. Pettit *et al*. [8], also conducted a corrosion test of YSZ in $NaVO_3$ and found that a porous layer is formed over the YSZ surface. Hence, it is clear that corrosion of ZrO_2 results from de-stabilization due to the molten salt. Thus, it is necessary to find oxides with low reactivities with molten salts, to be used as stabilizing agents for ZrO_2 ceramics [13].

Al_2O_3 ceramics have high melting points and are stable but do not have phase transitions at high temperatures like the ZrO_2 ceramics further they have small solubilities in molten salts and are expected to show excellent corrosion resistance [14, 15]. However, Pettit *et al*. [8], have found that a porous layer is formed over the surface of Al_2O_3 when it is exposed to the molten salt of Na_2SO_4-$NaVO_3$. They reported that this layer increases with increasing concentration of V_2O_5 in the molten salt. Furthermore, they conducted a corrosion test on Al_2O_3 of various purities in Na_2SO_4 [15] and found that impurities existing in grain boundary regions affect the corrosion resistance of the ceramics. Yoshiba *et al*. [10], also showed that the purity of Al_2O_3 affects corrosion resistance to molten salt. Since this porous layer can cause the strength of Al_2O_3 to decrease, it must be minimized: however, because it forms on Al_2O_3 ceramics which have a relatively high purity, it would be difficult to further improve the corrosion resistance of Al_2O_3 alone. The combination of Al_2O_3 with another type of ceramic may be useful method to improve corrosion resistance of the Al_2O_3 ceramics.

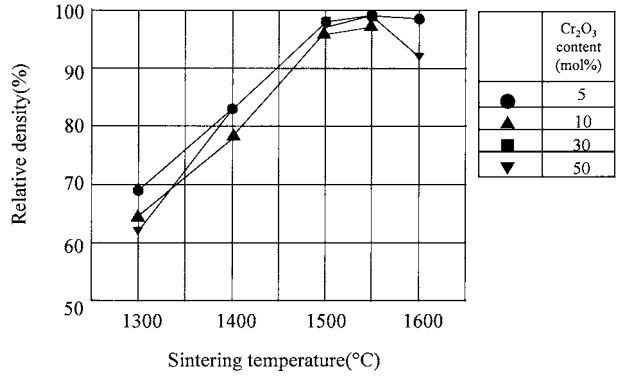

Figure 1 Relationship between relative density of Cr_2O_3-Al_2O_3 ceramics and sintering temperature.

TABLE I Chemical composition of powders

Powder	Chemical composition (%) Cr_2O_3	SO_4	Ig.loss	Average diameter (μm)
Cr_2O_3	99.4	0.3	0.3	0.2

Powder	Chemical composition (ppm) Na	K	Ca	Mg	Fe	Si	Ga	Cr	Average diameter (μm)
Al_2O_3	15	5	2	1	4	6	2	2	0.25

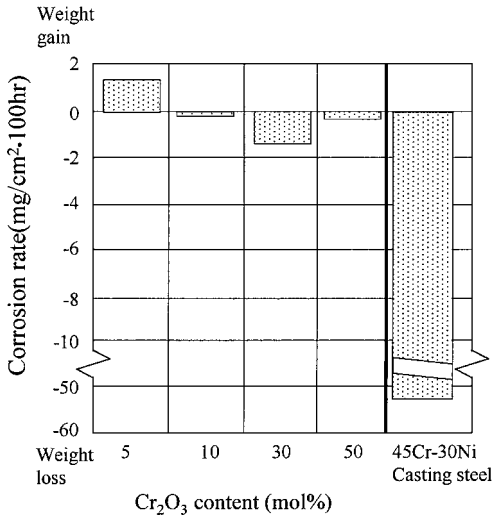

Figure 2 Dependence of corrosion rate on Cr_2O_3 content in Cr_2O_3-Al_2O_3 sintered bodies (Sintering temperature: 1550°C, Testing conditions: Temperature: 900°C).

Cr_2O_3 has a crystal structure similar to that of Al_2O_3 and is completely soluble on Al_2O_3 [16]. It may be a suitable addition as it has been used as one of the constituents to improve the corrosion resistance of oxide refractories [17]. It has been reported that addition of Cr_2O_3 would enhance corrosion resistance due to a decreased solubility and increased viscosity of the molten oxides [18], and hence, this combination can be expected to show a high corrosion resistance to the molten salt as well.

The results of an examination of the effect of addition of Cr_2O_3 to Al_2O_3 in order to improve the high-temperature corrosion resistance in molten Na_2SO_4-V_2O_5 are presented here.

2. Experimental procedures

The material used were Cr_2O_3 powder (purity 99.4%, mean particle size 0.2 μm, Nihon Kagaku Kogyo,

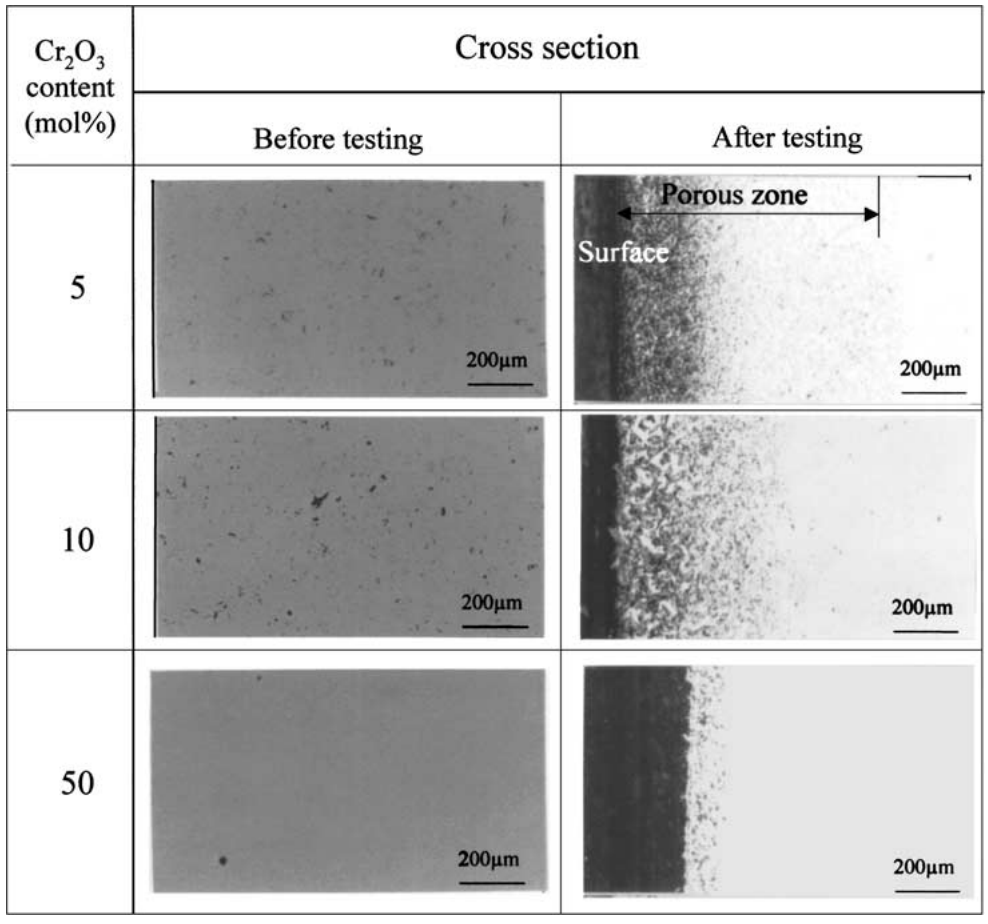

Figure 3 Cross section of Cr_2O_3-Al_2O_3 ceramics (Sintering temperature: 1500°C).

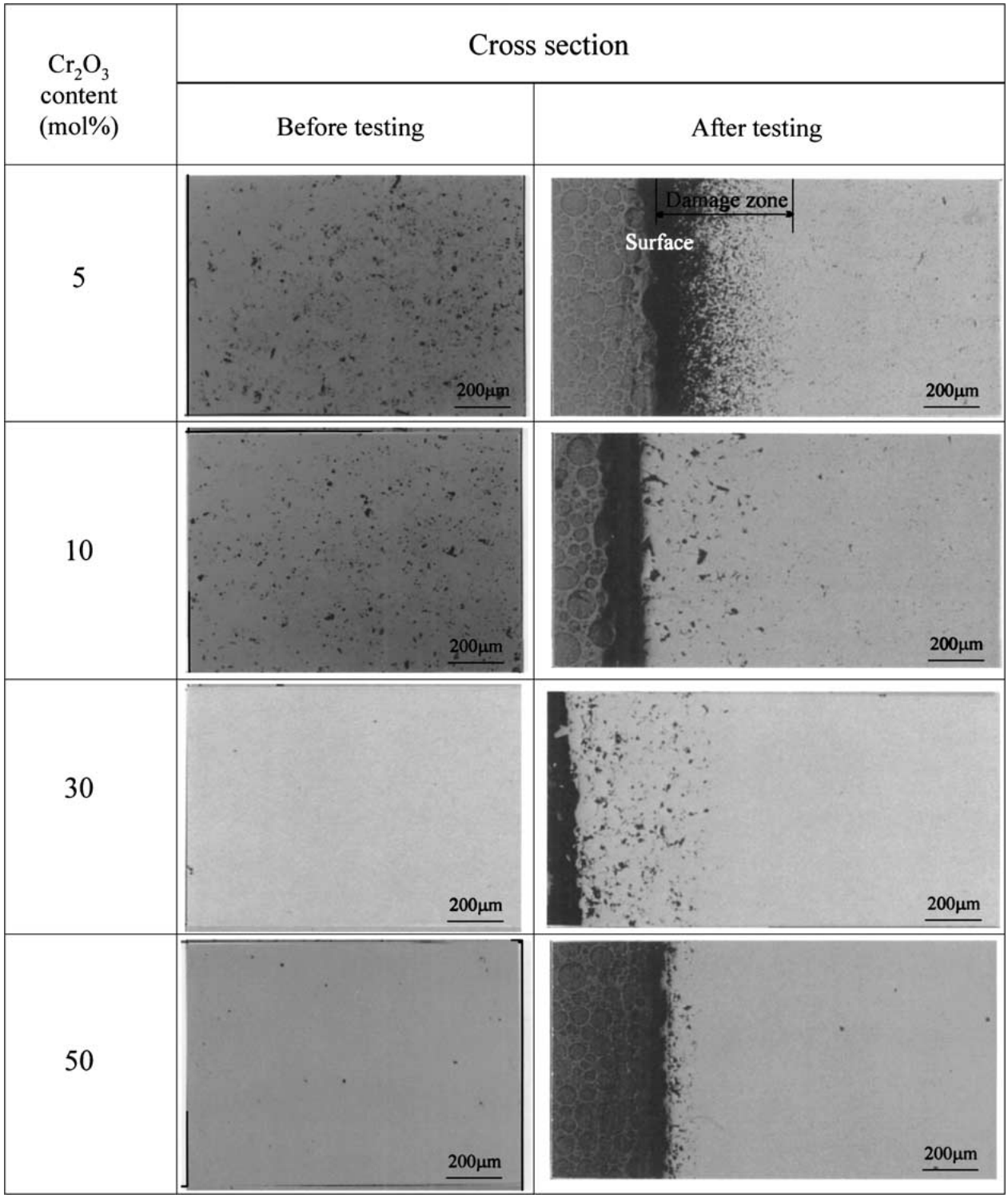

Figure 4 Cross section of Cr_2O_3-Al_2O_3 ceramics (Sintering temperature: 1550°C).

Ltd., Kromex A-1) and Al_2O_3 powder (purity 99.997%, mean particle size 0.25 μm, Showa Denko, Ltd., UA-5105). Properties of the material powders are listed in Table I. These powders were mixed in ethanol together with a small amount of an additive for homogenous mixing. The mixture of the powders and ethanol was dried in an oven at 80°C. The powder obtained was pressed as discs shaped measuring approximately 20 mm in diameter and 5 mm in thickness. These were sintered in a vacuum of 10^{-2} torr at various temperatures. The density of the sintered body was calculated from its weight and volume.

For the high-temperature corrosion test, specimens measuring 15 mm in diameter and 5 mm in thickness were cut from the sintered body. The surface of the test specimen was polished to a mirror finish using diamond paste with a mean particle size of 1 μm. The test specimen was placed in a crucible containing 25 grams of salt consisting of 60wt%V_2O_5-40wt%Na_2SO_4. The crucible used was made of Al_2O_3 of the highest purity commercially available (purity 99.7%, SSA-S grade, Nikkato, Ltd.). 12.5 grams of the salt was placed in the crucible, the test specimen was placed on the salt parallel to the bottom of the crucible and another 12.5 grams

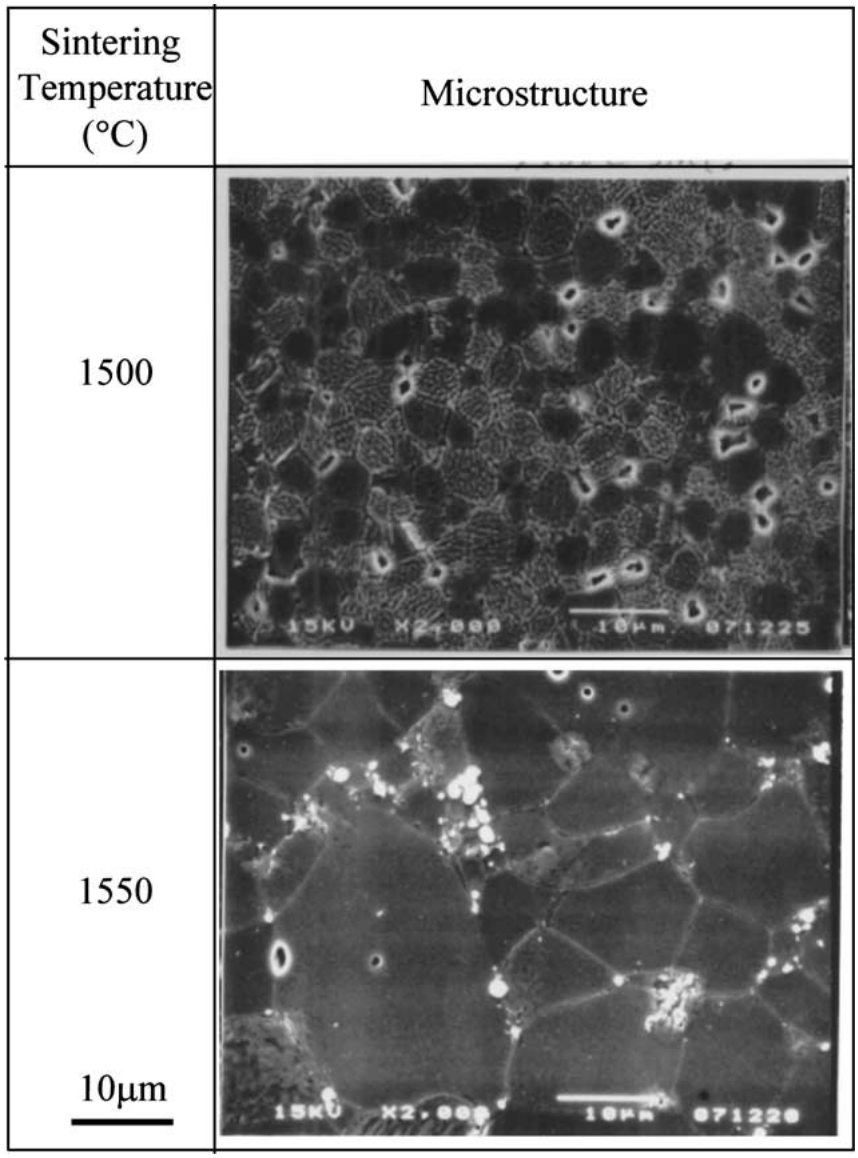

Figure 5 Microstructure of 50 mol% Cr_2O_3-Al_2O_3 ceramics before testing.

of the salt was placed on the specimen. The crucible containing the salt and the test specimen was covered with its lid and heated in an atmospheric furnace at 900°C for 100 hours. Sulphur in the molten salt escaped as either SO_2 or SO_3, leaving Na and V only in the molten salt after testing. The test specimen was taken from the crucible, and cleaned using water at 80°C for 48 hours.

After testing, the weight change of the test specimen was measured and the corrosion layer thickness was measured using an optical microscope (Olympus Ltd., Model: VANOX-T). Microstructures of the test specimens were observed using Scanning Electron Microscopy (SEM, JEOL Ltd., Model: JSM-T330A) and Transmission Electron Microscopy (TEM, JEOL Ltd., Model: JEM-2000FXII). Also, distributions of component elements of the salt were analyzed using an Electron Probe Micro Analyzer (EPMA, JEOL Ltd., Model: JXA-8600).

3. Results and discussion

Fig. 1 shows the relationship between the sintering temperature and the sintered density of the Cr_2O_3-Al_2O_3 ceramics. The relative density of the Cr_2O_3-Al_2O_3 ceramics increased with increasing sintering temperature. The relative density exceeded 95% a sintering temperature of 1500°C.

Fig. 2 shows the relationship between the post-test weight change of the Cr_2O_3-Al_2O_3 ceramics and the Cr_2O_3 addition. The weight change per unit area was relatively small and appeared not to depend on the level of the Cr_2O_3 addition. For example, for 50mol% Cr_2O_3-Al_2O_3, the sintered product at 1550°C shows a weight loss of 0.77 mg/cm^2 and this corresponds to removal of about 10 μm.

Figs 3 and 4 show the pre-test microstructural observations of specimens sintered at 1500°C and at 1550°C. The sintered compacts of 5mol%Cr_2O_3-Al_2O_3 and 10mol%Cr_2O_3-Al_2O_3 showed slight porosity at any of the sintering temperatures. Fig. 5 shows microstructures of the 50mol%Cr_2O_3-Al_2O_3 ceramics prepared by sintering at 1500°C and at 1550°C. The grain size at 1500°C was about 10 μm whereas the grain size at 1550°C was as large as about 30 μm, but no abnormal grain growth was discerned.

Figs 3 and 4 show the post-test microstructural observations of the test specimens sintered at 1500°C and at

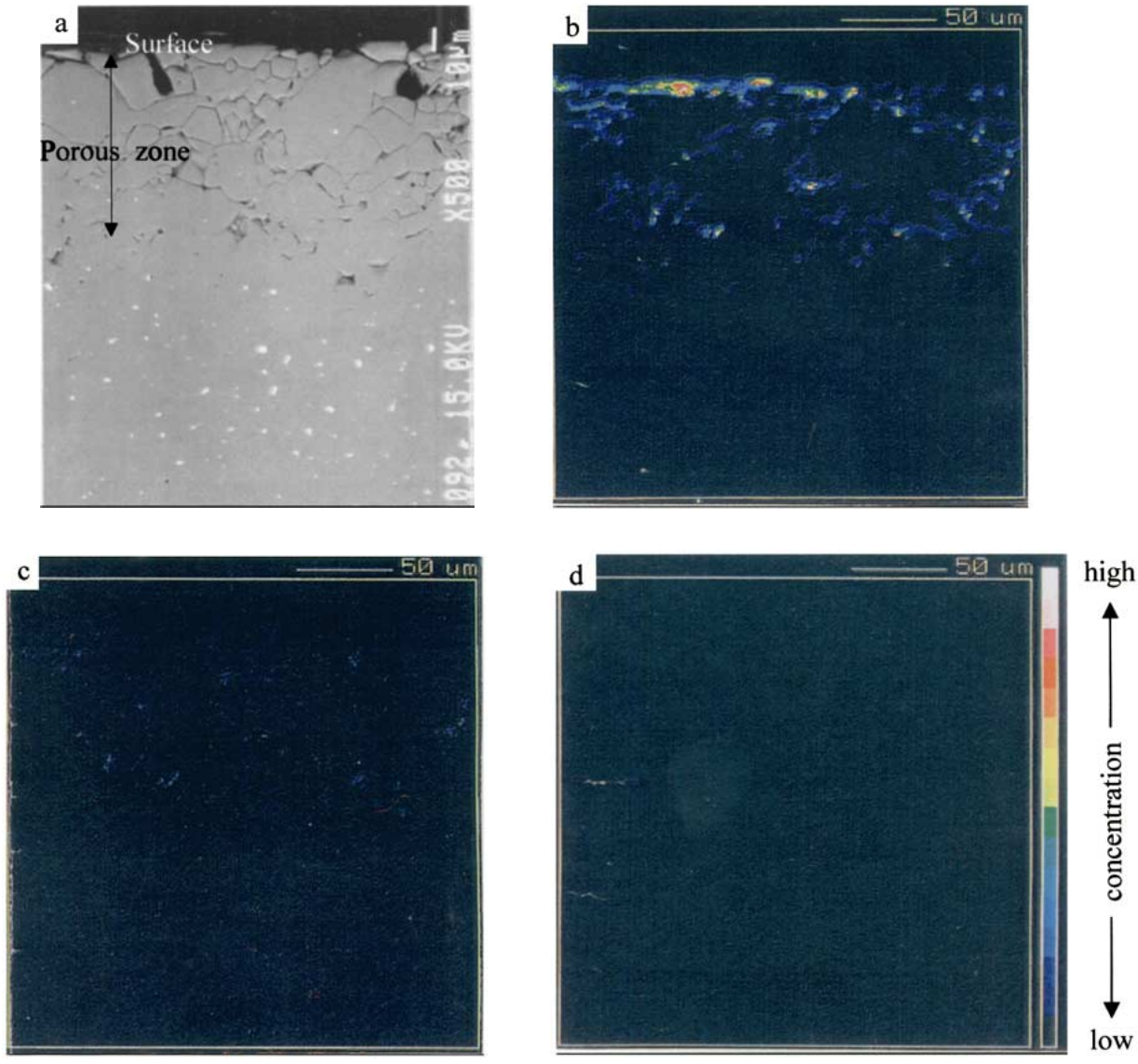

Figure 6 Cross section and distribution of elements in a Cr_2O_3-Al_2O_3 specimen after corrosion test (a) Backscatter image; (b) V map; (c) Na map and (d) S map, 50 mol% Cr_2O_3-Al_2O_3, Sintering temperature: 1550°C).

1550°C. After corrosion testing, a porous layer covering all the surfaces of the test specimens was discerned. Also, the thickness of the porous layer decreased with increasing addition of Cr_2O_3. Furthermore, the thickness of the porous layer in the test specimen sintered at 1550°C was smaller than that of the same composition test specimen sintered at 1500°C.

Fig. 6 shows the microstructural observation of the porous layer and the distribution of the molten salt components in this layer. In this region, distinct grain boundaries could be observed and V and Na were detected in the grain boundary region. It is inferred that this porous layer is a product caused by corrosion as pointed out by Pettit *et al*. [6], and that the constitutions of the molten salt penetrate along the grain boundary into the test specimen.

Fig. 7 shows the TEM observation of grain boundaries in the area right beneath the porous layer of the 50mol%Cr_2O_3-Al_2O_3 ceramic sintered at 1550°C. As seen from Fig. 7, a phase consisting of V and Na was observed in the grain boundary regions. Some grain boundary regions in which there was an absence of these elements were also found. Therefore, there is mixture of grain boundaries, beneath the porous layer. Si was not detected within these grain boundaries. Pettit *et al*. [6], examined the corrosion behavior in Na_2SO_4 of Al_2O_3 ceramics of different purities and inferred that intergranular corrosion can be caused by the selective corrosion of an alumino-silicate phase existing in the grain boundaries. However, in the present study it is unlikely that the corrosion was caused by dissolution of a grain boundary phase, because Si was absent from the grain boundaries. Fig. 8 shows a phase diagram of $NaVO_3$ (V_2O_3-Na_2O)-Al_2O_3 [19]. As seen from this figure, $NaVO_3$ and Al_2O_3 produce a liquid phase at a low temperature. From this phase diagram, it is inferred that a liquid phase of V_2O_5-Na_2O-Cr_2O_3-Al_2O_3 is also produced in grain boundaries. In Fig. 9, a grain boundary containing V and Na is shown. The grain adjacent to the grain boundary has ledges. Therefore, V_2O_5 and Na_2O that have reached the grain boundary continue to penetrate further while producing liquid phase.

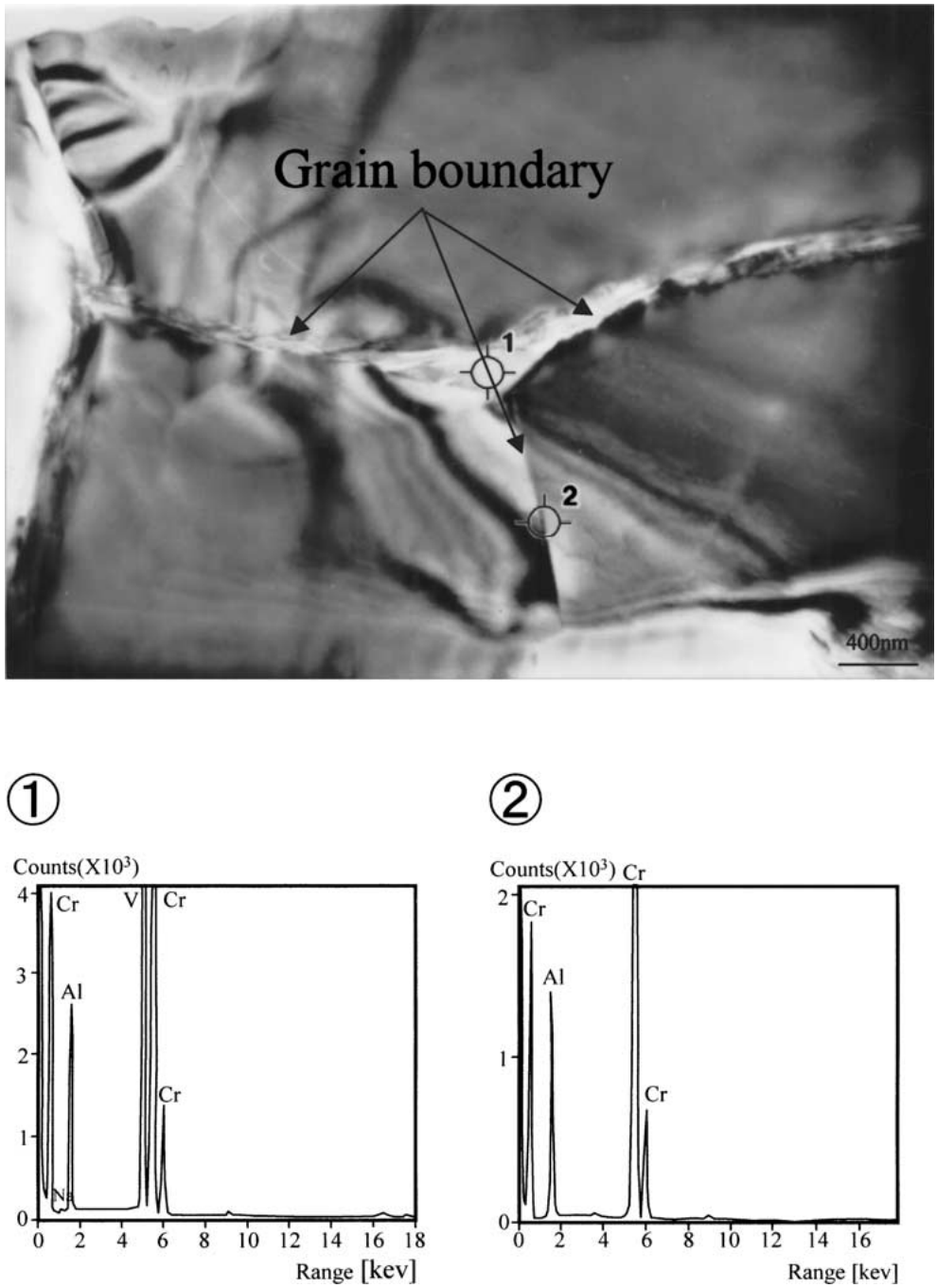

Figure 7 Microstructure and EDS analysis of 50 mol% Cr_2O_3-Al_2O_3 ceramics after corrosion test.

To clarify the corrosion mechanism, the dependence of holding time on corrosion was evaluated. The test was conducted at 900°C. In addition to 50mol%Cr_2O_3-Al_2O_3, the pure Al_2O_3 which was sintered at 1550°C was also evaluated for comparison.

From Fig. 10, it can be seen that the corrosion layer thickness of the pure Al_2O_3 is proportional to the holding time whereas that of the 50mol%Cr_2O_3-Al_2O_3 is proportional to 0.5 power of the holding time. It is, therefore, inferred that the corrosion reaction of the Al_2O_3 is controlled by the rate of reaction whereas the corrosion reaction of Al_2O_3-Cr_2O_3 is controlled by the rate of diffusion [20]. As discussed above, it is inferred that corrosion proceeds due to dissolution of the grain boundary regions into the liquid phase. In the case of Al_2O_3-Cr_2O_3, it is inferred that this dissolution of the grain boundary regions into the liquid phase follows the rate control of the external diffusion of the grain constituents or of the internal diffusion of the molten salt constituents, which causes the dissolution rate to decrease with increasing thickness of the corrosion layer. Furthermore, it is inferred that because of this, the corrosion rate can decrease with increasing addition of Cr_2O_3 in Al_2O_3-Cr_2O_3. It has been reported that if Cr_2O_3 is added to refractory in contact with molten oxides, an increased viscosity of the oxides can decrease the diffusion rate of the refractory constituents into the molten oxides, which in turn, can improve corrosion resistance of the refractory [18]. In the present study, therefore, it is also inferred that the viscosity of the liquid phase which penetrated into the sintered bodywas raised by dissolution of Cr_2O_3 to decrease the

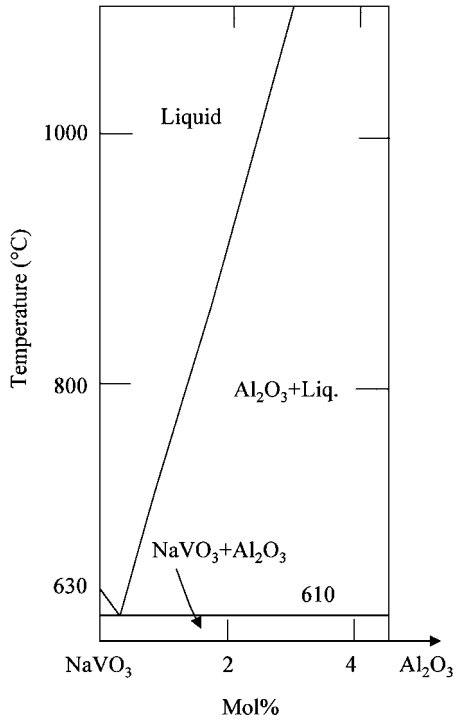

Figure 8 Phase diagram of $NaVO_3$ (Na_2O-V_2O_5)-Al_2O_3.

diffusion rate of the grain constituents or the molten salt constituents, which in turn, decreased the dissolution rate with increasing thickness of the corrosion layer. Also, from Figs 3 and 4, the corrosion resistance can be enhanced by increasing the sintering temperature. Fig. 5 shows that the grain size increases with increasing sintering temperature, and it is inferred that this could improve the corrosion resistance.

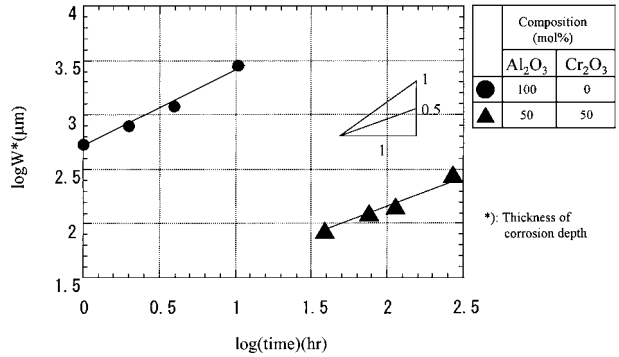

Figure 10 Relation between the thickness of corrosion depth and time (Sintering temperature: 1550°C, Testing conditions: Temperature: 900°C).

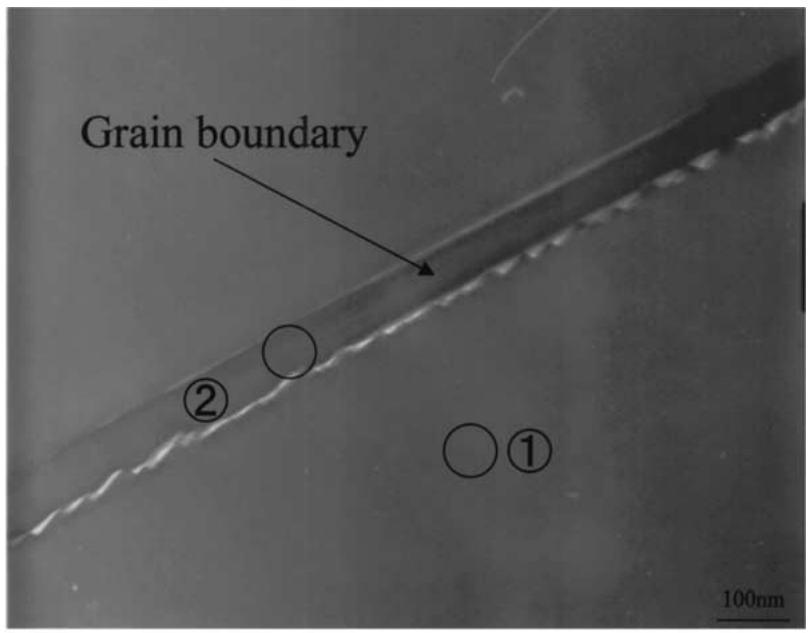

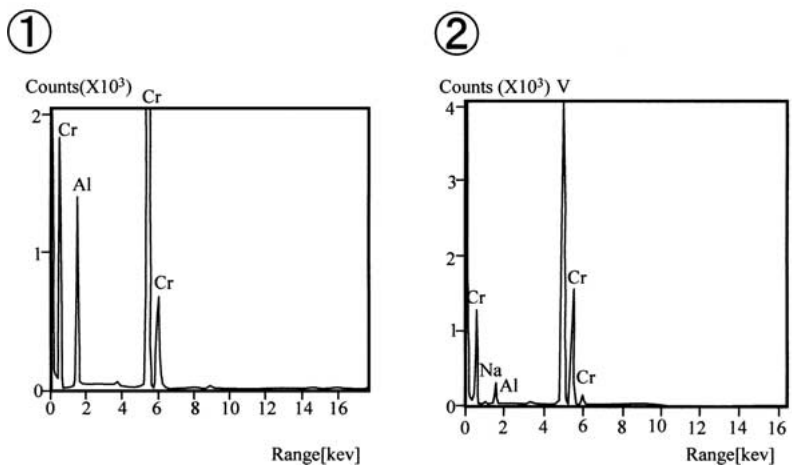

Figure 9 Microstructure and EDS analysis of 50 mol% Cr_2O_3-Al_2O_3 ceramics after corrosion test.

4. Conclusions

1. Addition of Cr_2O_3 to Al_2O_3 forms the solid solution of $(Al,Cr)_2O_3$ and improves the high-temperature corrosion resistance of Al_2O_3. The thickness of the corrosion layer depends on the sintering temperature and the addition level of Cr_2O_3.

2. Corrosion of the Cr_2O_3-Al_2O_3 ceramics is caused by the formation of a liquid from the Na_2O-V_2O_5-$(Al,Cr)_2O_3$ system and by dissolution of the Cr_2O_3-Al_2O_3 ceramics into this liquid.

3. It is inferred that the corrosion rate of the Cr_2O_3-Al_2O_3 ceramics is lower than that of the Al_2O_3 ceramics because the dissolution rate of grains into the liquid phase occurring in the grain boundaries is decreased, compared with the Al_2O_3 ceramics.

4. If the sintering temperature is raised, grain growth occurs which could enhance the corrosion resistance of the ceramics.

References

1. R. M. PERSOONS, in Proceedings of the NATO Advanced Research Workshop on Corrosion of Advanced Ceramics, edited by K. G. Nickel (Kluwer Academic Publishers, 1993) p. 297.
2. N. S. JACOBSON, *J. Amer. Ceram. Soc.* **76** (1993) 3.
3. T. SATO, Y. KOIKE, T. ENDO and M. SHIMADA, *J. Mater. Sci.* **23** (1988) 1405.
4. W. C. SAY and S. C. LIU, *ibid.* **31** (1996) 3003.
5. D. W. McKEE and P. A. SIEMERS, *Thin Solid Films* **73** (1980) 439.
6. R. J. BRATTON and S. K. LAU, in Proceedings of the International Conference on the Science and Technology of Zirconia, Cleveland (The Amer. Ceram. Soc., 1981), p. 226.
7. H. WATANABE and M. CHIGASAKI, *Yogyo-Kyokai-Shi* **92** (1984) 308.
8. F. S. PETTIT, G. H. MEIER and J. R. BLACHERE, in Proceedings of the NATO Advanced Research Workshop on Corrosion of Advanced Ceramics, edited by K. G. Nickel (Kluwer Academic Publishers, 1993) p. 235.
9. R. L. JONES, *J. Electrochem. Soc.* **133** (1986) 227.
10. M. YOSHIBA and H. WADA, "High Temperature Corrosion of Advanced Materials and Protective Coatings" (Elsevier Science Publishers, London, 1992) p. 355.
11. Y. HARADA, M. YOSHIBA, T. ARANAMI and H. TAIRA, in Proceedings of Thermal Spraying, Kobe, Japan, May 1995 (High Temperature Society of Japan, 1995) p. 89.
12. H. YAMAMOTO, S. ONO, H. TSUNODA and H. MOTOMURA, *Mitsubishi Jyuko Giho* **25** (1988) 25.
13. R. L. JONES, *Surface and Coatings Technology* **39/40** (1989) 89.
14. R. A. RAPP, "High-Temperature Chemistry" (Elsevier Science Publishers, New York, 1989) p. 291.
15. F. S. PETTIT, *J. Mater. Res.* **8** (1993) 1964.
16. E. N. BUNTING, *Bureau of Standards Journal of Research* **6** (1931) 947.
17. A. E. THOMAS, *J. Canadian Ceramic Society* **45** (1976) 21.
18. M. NAKAMURA, in Proceedings of the 7th International Symposium on Ultra-High Temperature Materials '97 in Tajimi (The Committee Meeting of the 7th International Symposium on Ultra-High Temperature Materials, 1997), p. 73.
19. L. A. KLINKOVA and E. A. UKSHE, *Zh. Neorg. Khim.* **20**(2) (1975) 481.
20. R. E. TRESSLER, in Proceedings of the NATO Advanced Research Workshop on Corrosion of Advanced Ceramics, edited by K. G. Nickel (Kluwer Academic Publishers, 1993) p. 3.

Received 3 November 1999
and accepted 10 August 2001